J Mater Sci (2006) 41:4713–4719
DOI 10.1007/s10853-006-0057-0

$La_{1-x}A'_xCo_{1-y}Fe_yO_{3\pm\delta}$ (A′ = Ce,Sr) catalysts for the flameless combustion of methane

E. Campagnoli · A. C. Tavares · L. Fabbrini · I. Rossetti · Yu. A. Dubitsky · A. Zaopo · L. Forni

Received: 21 December 2004 / Accepted: 22 September 2005 / Published online: 27 April 2006

Abstract A set of $La_{1-x}A'_xCo_{1-y}Fe_yO_{3\pm\delta}$ samples (A′ = Ce,Sr; $x = 0.1, 0.4$, $y = 0, 0.5, 0.8, 1$) was prepared by means of the sol–gel citrate method and characterised through X-ray diffraction (XRD), N_2 adsorption/desorption and temperature programmed desorption–reduction (TPD-TPR). Their activity for the catalytic flameless combustion of methane was tested and the results interpreted focusing on the effect of doping at A and/or B position. It was found that Ce doping of lanthanum ferrite catalysts could suppress suprafacial activity and slightly enhance intrafacial activity, due to the change of oxygen mobility. However, catalytic activity seems independent of the type of electronic conductivity (*p*- or *n*-type), the activity of an analogously Sr-doped sample being similar to that of the Ce-doped one. Mixed B-metal composition can help in modulating both oxygen mobility and catalyst stability under reducing reaction conditions. High Fe content allows to optimise this last parameter. However, depression of oxygen mobility and hence of activity has to be prevented by proper doping at A-position.

Introduction

The catalytic flameless combustion (CFC) of hydrocarbons is an efficient method for limiting or even suppressing the formation of harmful pollutants during combustion, being carried out at considerably low temperature (ca. 800 °C). Perovskite-like materials proved to be interesting catalysts for this reaction, being cheaper, comparatively active and much more resistant to deactivation than the traditional noble metal based catalysts.

Perovskites are mixed oxides of general formula ABO_3, where both A and B metal ions can be partially substituted, leading to a wide variety of compounds. These are often characterised by oxygen non-stoichiometry, which determines interesting catalytic properties for many reactions [1, 2]. If the B position is occupied by a first-row transition metal ion these oxides are semiconductors possessing a relatively high electronic conductivity. In particular, the nature and amount of a substitute A′ at A position can stabilise unusual oxidation states for the B cation, the responsible of the catalytic action, and/or generate anionic vacancies in the solid [3].

Perovskites as oxidation catalysts act through two different mechanisms, called *suprafacial* and *intrafacial*, involving adsorbed or bulk oxygen, respectively [4]. Oxygen mobility is tightly connected with the presence of oxygen vacancies: the higher their concentration, the lower is the activation barrier for oxygen transport. So, it can be expected that ionic mobility and hence intrafacial activity would be enhanced by proper doping. Summarising, the main requirements to ensure high catalytic activity for CFC of methane are high electronic conductivity, both of *p*- or *n*-type, together with anion lattice disorder, which favours oxygen migration [5].

Undoped ABO_3 perovskites are usually rather active through the suprafacial mechanism [1], due to the low ionic mobility across the crystal lattice. By contrast, high ionic mobility favours the participation of bulk oxygen, typical of the intrafacial mechanism.

E. Campagnoli · L. Fabbrini · I. Rossetti · L. Forni (✉)
Dipartimento di Chimica Fisica ed Elettrochimica, Università degli Studi di Milano, Via Golgi, 19 I-20133 Milano, Italy
e-mail: lucio.forni@unimi.it

A. C. Tavares · Yu. A. Dubitsky · A. Zaopo
Pirelli Labs SpA, V.le Sarca, 222 Milano, Italy

In general the partial substitution of A with an A′ cation of lower valence leads to the formation of oxygen vacancies and enhances ionic conductivity [6]. However, in the case of lanthanum based materials (A = La), the effect of this substitution can vary, depending on the nature of B ion.

In the recent past we have reported interesting catalytic properties of $La_{0.9}Ce_{0.1}CoO_{3\pm\delta}$ for the title reaction, both in powder and in honeycomb-supported form [7–9]. Indeed, hetero-valent ion substitution for La-cobaltites brought about a considerable increase in catalytic activity for Ce(IV) doped samples, while lower activity was observed for Sr(II) or Eu(II) doped catalysts [8, 10]. The electric charge disequilibrium, consequence of Ce(IV) partial substitution for La(III), is compensated by the reduction of some Co(III) to Co(II) and/or by a decrease of anionic vacancies concentration. Gaseous oxygen can be reduced on Co(II) sites, which are then oxidised back to Co(III) and the formation of paramagnetic pairs such as Co(III)/O_2^- found evidence through electron paramagnetic resonance (EPR) analysis [8]. On the other hand, La(III) substitution by a bivalent cation (e.g. Sr^{2+} or Eu^{2+}) favours Co(III) oxidation to Co(IV) and the subsequent reduction of the latter is favoured, accompanied by oxygen release from the bulk. The net result is an increase of anionic vacancies. In principle this could enhance catalytic activity, at least through the suprafacial mechanism, but the experimental evidence was a lower methane conversion with respect to the Ce-doped sample. A possible explanation has been suggested as connected with the formation of spin-glass, observed in $La_{0.9}Sr_{0.1}CoO_{3-\delta}$, which would account for the low oxygen exchange ability of the sample and therefore for its lower activity with respect to the Ce-doped homologue, where spin-glass systems were not observed [11].

Moreover, an investigation on undoped $LaBO_3$ samples showed similar activity for the ferrite and the cobaltite catalysts, the main difference being the strong suprafacial activity of the former [12]. Indeed, $LaFeO_3$ showed ca. 30% CH_4 conversion below 400 °C. This behaviour was explained on the basis of the lower ion mobility within the undoped perovskites, favouring mainly the reaction though the low-temperature suprafacial mechanism. A confirmation was found through temperature programmed desorption (TPD) experiments [12].

Recently, $La_{1-x}Sr_xCo_{1-y}Fe_yO_{3-\delta}$ materials gained attention due to their high mixed conductivity. Indeed, at high temperature (ca. 800 °C) their electronic conductivity can attain $10^2\ \Omega^{-1}\,cm^{-1}$, ionic conductivity ranging between 10^{-2} and $1\ \Omega^{-1}\,cm^{-1}$. For this reason their application was studied as cathodes for intermediate temperature solid oxides fuel cells (SOFCs) [13–15], as membranes for oxygen separation and for membrane reactors for syngas production and oxidation of hydrocarbons [16–19]. Moreover, $La_{1-x}Sr_xCo_{1-y}Fe_yO_{3-\delta}$ materials are reported to absorb and release high amounts of oxygen and vacancies formation and oxygen absorption properties of these perovskites are tightly bound to the substitution degree x.

The aim of the present work was then to prepare a set of $La_{1-x}A'_xCo_{1-y}Fe_yO_{3\pm\delta}$ samples (A′ = Ce, Sr; x = 0.1, 0.4; y = 0, 0.5, 0.8, 1), to characterise and to test them for the CFC of methane, in order to check the effect of doping at A or B position on catalyst performance, as well as on some interesting physical–chemical properties.

Experimental

Catalyst preparation

All the present samples were prepared through the sol–gel method, by using citric acid as complexing agent. Proper amounts of the precursor salts, $La(NO_3)_3{\cdot}6H_2O$, $Ce(NO_3)_3{\cdot}6H_2O$, $Sr(NO_3)_2$, $Fe(NO_3)_3{\cdot}9H_2O$, $Co(NO_3)_2{\cdot}6H_2O$, were dissolved in deionised water and mixed with an aqueous solution of citric acid. Water was evaporated in vacuo (50 °C, 25 Torr residual pressure, 1 Torr = 133 Pa) and the gel so obtained was dried for 7 h (70 °C, 35 Torr residual pressure). The dry solid was then calcined in air, heating by 0.5 °C/min till 140 °C, then by 1 °C/min up to 700 °C. Further calcination up to 950 °C and 1100 °C was carried out on sample $La_{0.6}Sr_{0.4}Fe_{0.8}Co_{0.2}O_{3-\delta}$. The composition and some relevant physical properties of the samples prepared are reported in Table 1.

Catalyst characterisation

BET specific surface area was determined by N_2 adsorption–desorption, by means of a Micromeritics ASAP 2010 instrument. The crystalline phases were recognised through powder X-ray diffraction (XRD) by means of a Philips PW1820 diffractometer, by using the Ni filtered Cu Kα radiation (λ = 1.5418 Å) and comparing the patterns obtained with literature data [20]. Crystallite dimension was calculated by the Scherrer equation applied to the main reflections of the XRD pattern.

Temperature programmed desorption-reduction (TPD-TPR) analysis

The apparatus and procedure were described elsewhere [12, 21]. Briefly, ca. 0.20 g of catalyst were loaded into a continuous, tubular quartz microreactor, fed with 20 cm^3/

Table 1 Catalyst composition and main physical and catalytic properties

Sample	Composition	d (nm)[a]	BET_{SSA} (m^2/g)	$T_{1/2}$ (°C)	T_f (°C)
LCC	$La_{0.9}Ce_{0.1}CoO_{3\pm\delta}$	20	13.6	415	497
LCF	$La_{0.9}Ce_{0.1}FeO_{3\pm\delta}$	26	11.6	408	495
LCFC	$La_{0.9}Ce_{0.1}Fe_{0.5}Co_{0.5}O_{3\pm\delta}$	17	13.8	400	504
LSFC	$La_{0.6}Sr_{0.4}Fe_{0.8}Co_{0.2}O_{3-\delta}$	14	18.3	400	484
LSFC950 [b]	$La_{0.6}Sr_{0.4}Fe_{0.8}Co_{0.2}O_{3-\delta}$	16	3.6	448	541
LSFC1100 [c]	$La_{0.6}Sr_{0.4}Fe_{0.8}Co_{0.2}O_{3-\delta}$	/	<0.5	490	603

[a]From XRD data calculated through the Scherrer equation [J.R. Anderson, K.C. Pratt, ''Introduction to characterisation and testing of catalysts'', Academic Press, New York, 1985]

[b]Calcined at 950 °C

[c]Calcined at 1100 °C. $T_{1/2}$ = methane 50% conversion temperature. T_f = methane 100% conversion temperature

min of super-pure He (purity ≥99,9999 vol%) and heated by an electric furnace, controlled by an Eurotherm 2408 TRC. The composition of the outlet gas was analysed by means of a quadrupolar mass spectrometer (QMS) (MKS, PPT Residual Gas Analyser). TPD of pre-adsorbed O_2 was carried out in 20 cm^3/min flowing He, after overnight saturation in 20 cm^3/min flowing air (purity ≥99,9995 vol%) at 750 °C and back to 50 °C, always in flowing air. Prior to desorption the sample was equilibrated in 20 cm^3/min flowing He at 50 °C, then heated (10 °C/min) up to 800 °C. A further TPD experiment was carried out to check for the possible adsorption-direct transformation of the hydrocarbon. CH_4 was isothermally fed at different temperatures (50, 100, 200, 500 and 600 °C) by flowing 30 cm^3/min of a mixture of 1.04 vol% CH_4 in He for 1 h. The subsequent TPD run was carried out following the above-described procedure. Finally, a TPR experiment was carried out by feeding continuously 30 cm^3/min of the same CH_4 in He gas mixture through a sample pre-saturated in 20 cm^3/min flowing air at 750 °C for 1 h, then heated (10 °C/min) up to 650 °C.

Catalytic activity

The activity for the CFC of methane was measured by means of a bench scale continuous apparatus. Standard reaction conditions were as follows: 0.2 g of catalyst, diluted with 1.3 g of quartz, both in 0.15–0.25 mm particle size, were loaded into a tubular quartz reactor (7 mm i.d.), heated by an electric furnace, controlled by an Eurotherm 812 TRC. The catalyst was activated in flowing air (20 cm^3/min), while increasing temperature (10 °C/min) up to 650 °C, then kept for 1 h. After cooling in flowing air down to 250 °C, the gas flow was switched to a mixture of 10 cm^3/min of 1.04 vol % CH_4 in He + 10 cm^3/min of air. The gas flow rates were regulated by means of MKS 1259 mass flow-meters, governed by a MKS 247 control unit. The temperature was increased (2 °C/min) up to 650 °C, while monitoring methane conversion by means of an in-line HP 5890 A gas chromatograph, equipped with a thermal-conductivity detector (TCD).

Results and discussion

Calcination-milling, sol–gel procedure, flame-hydrolysis and reactive grinding are useful methods for obtaining oxides with different properties [22]. However, the preparation procedure not only influences surface area, particle size, morphology and crystal structure, but also affects electric and diffusional properties, which are parameters of interest for the present reaction. Indeed, a comparison analysis showed *e.g.* that the sol–gel citrate prepared samples were characterised by a much higher electronic conductivity and slightly higher ionic conductivity than those obtained by the solid state procedure [19]. Then, to avoid the possible complication brought about by the use of different preparation methods, the sol–gel citrate procedure was adopted here for catalyst preparation, followed by calcination at 700 °C. This allowed to obtain samples with BET specific surface area (BET_{SSA}) between 10 and 15 m^2/g almost independently of their composition (Table 1, samples LCC, LCF, LCFC). A slightly higher value was observed for the LSFC sample, which, however, when calcined at higher temperature, i.e. 950 °C and 1100 °C, transformed into a material with progressively much lower BET_{SSA}.

High phase purity was obtained for every sample, as revealed by the XRD analysis [20]. An exception was again sample LSFC, showing also very weak reflections due to $SrCO_3$, which however disappeared after calcination at 950 °C (Fig. 1). The largest crystal size was observed in sample LCF, the smallest in sample LSFC. The latter maintained a very low crystal size even after calcination at 950 °C, in spite of the evident decrease of BET_{SSA} (Table 1).

All the present samples proved to be very active for the CFC of methane (Table 1 and Fig. 2), most of them leading to full conversion of the paraffin at $T_f < 500$ °C, T_f

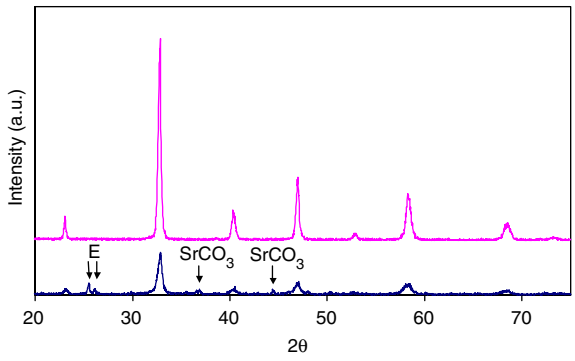

Fig. 1 XRD pattern of sample $La_{0.6}Sr_{0.4}Fe_{0.8}Co_{0.2}O_{3-\delta}$ calcined at increasing temperature: LSFC (lower pattern); LSFC950 (upper pattern) (Table 1). E = undetermined impurity

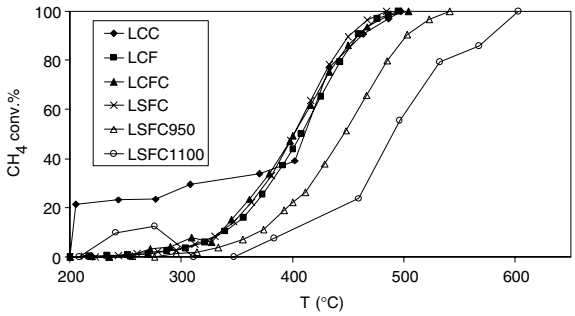

Fig. 2 Catalytic activity data for the CFC of methane

being the temperature at which, during the activity test run, methane conversion attains 100%.

Effect of substitution at A-site

A similar high temperature intrafacial activity was noticed for LCC and LCF samples (Fig. 2). However, the catalytic behaviour at low temperature was opposite with respect to the undoped ABO_3 samples, as reported for $LaFeO_{3\pm\delta}$ and $LaCoO_{3\pm\delta}$ [12]. Indeed, $LaFeO_{3\pm\delta}$ showed the highest suprafacial activity [12], while $La_{0.9}Ce_{0.1}FeO_{3+\delta}$ proved much less active at such temperatures. On the other hand, $La_{0.9}Ce_{0.1}CoO_{3+\delta}$ showed a relatively high suprafacial activity, reaching 20% methane conversion at temperature as low as 200 °C [8, 9].

The different behaviour of the undoped $LaFeO_{3\pm\delta}$ (*suprafacial mechanism*) and $LaCoO_{3\pm\delta}$ (*intrafacial mechanism*) samples has been related to a lower oxygen mobility in the former with respect to the latter sample [12, 23, 24]. Oxygen mobility is tightly connected with the presence of oxygen vacancies: the higher their concentration, the lower is the activation barrier for oxygen transport. High ionic mobility favours the participation of bulk oxygen, typical of the intrafacial mechanism. According to the reported results, the Ce doping in the present LCF sample very likely increased oxygen mobility with respect to the undoped sample, enhancing slightly the intrafacial activity and suppressing the suprafacial activity.

Though a direct comparison between these two sets of samples cannot be fully accurate, due to the different preparation procedure (SGC-method for the present samples and FH-technique for the undoped ones [12]), some points worth a discussion. In our opinion the reason of the inverted behaviour of doped and undoped samples can be searched not only in oxygen mobility, but also in the reducibility of the B-metal. Indeed, the methane CFC reaction mechanism includes a redox cycle involving gaseous oxygen and metal B in the perovskite framework. Ce(IV) substitution for La involves partial B(III) ion reduction to B(II) with a decrease of anionic vacancies concentration. As for ion reducibility, Co(III) reduction to Co(II) is easier than Fe(III) reduction to Fe(II). For instance, the reduction potentials for these redox couples in acidic solution are 1.92 V and 0.771 V, respectively, and the metal-oxygen binding energy is lower for Co than for Fe [25]. A further evidence is the absence of a β peak in the TPD pattern of $LaFeO_{3\pm\delta}$ up to a temperature as high as 800 °C, compared to the 750 °C onset temperature for $LaCoO_{3\pm\delta}$, this last parameter being usually assumed as an index of B metal reducibility [12]. In addition, catalytic activity can be generated through different mechanisms, depending on temperature and oxygen availability. Indeed, at low temperature reaction kinetics can be interpreted by a Rideal–Eley mechanism, in which adsorbed α oxygen can play an important role and surface area, together with oxygen vacancies concentration, are important parameters. On the other hand, at higher temperature bulk (or β) oxygen becomes reactive, reaction kinetics becomes of zero order with respect to gaseous oxygen partial pressure (pO_2) and surface area is no more of fundamental importance [26].

Furthermore, La substitution by Sr(II) leads to a *p*-type semiconductor, while a *n*-type material is obtained with Ce(IV). However, the role of holes as charge carriers is not clearly defined in the kinetics of methane oxidation. In addition, the effect of Sr doping on catalytic activity depends also on calcination temperature of the material. Indeed, Sr substitution for La increases activity for catalysts calcined at 850 °C, while activity decreases for calcination at 1200 °C. Then, generally speaking, *p*-type semiconductors seem to perform better. For instance, $La_{0.8}Sr_{0.2}FeO_{3-\delta}$, showing high ionic and low electronic conductivity [27, 28], is reported to be very active for the present reaction. Finally, some further parameters can influence catalytic activity, such as spin-glass formation.

Effect of substitution at B-site

Substitution of 50% Fe by Co (sample LCFC, Table 1) slightly improved catalytic activity at low temperature, leading to ca. 8% CH_4 conversion at 300 °C. The predominant reaction mechanism is intrafacial, as a result of the simultaneous presence of Ce at A-position and of Co at B-position.

The effect of La substitution was checked also with this catalyst type, by doping a sample with Sr (LSFC, Table 1). $La_{0.6}Sr_{0.4}Fe_{0.8}Co_{0.2}O_{3-\delta}$ belongs to an interesting class of materials, well characterised and used e.g. as cathodes for the intermediate temperature (500–700 °C) SOFCs, this composition representing a good compromise between stability and oxygen mobility.

Our LSFC sample, in spite of the presence of some $SrCO_3$ impurities (vide supra), revealed highly active for the CFC of methane, performing comparably to the previously described samples, but showing complete methane conversion at the lowest temperature (484 °C). Suprafacial activity was completely suppressed, Co content being lower, with respect to the LCFC sample, and the doping ion in A position being different. However, in spite of this, only a small difference in catalytic activity has been observed with respect to the LCFC sample at low temperature, the activity curves being almost perfectly overlapping (Fig. 2). A small increase of activity at high temperature, i.e. above 400 °C, can be observed when doping at A position with Sr in place of Ce. Further calcination of LSFC at 950 °C led to good phase purity and crystallinity (Fig. 1), however accompanied by a severe drop of BET_{SSA}. The result was a shift of methane conversion curve toward higher temperature (Fig. 2). The macroscopic decrease of catalytic activity can be partly connected with the decrease of surface area, but very likely this is not the main reason, because the predominant reaction mechanism is intrafacial. A concomitant reason can be searched in the increase of crystal size during overheating (Table 1), possibly leading to a different oxygen exchange ability. A similar but more dramatic result was obtained by treating the same sample at even higher temperature (1100 °C). The resulting sample was strongly sintered, with BET_{SSA} below the detection limit of our apparatus. However, its activity, though the lowest of the group, was sufficient to completely convert methane at ca. 600 °C (Fig. 2). Some suprafacial activity was observed for this sample, surely not due to oxygen adsorption on surface sites, due to the extremely low surface area. More likely, this low temperature contribution to activity could be due to oxygen vacancies formation occurring during treatment at so high temperature.

TPD-TPR analysis was carried out on our best-performing sample only (LSFC, Fig. 3). A first set of experiments aimed at investigating the possible adsorption and/or activation of the substrate. These were carried out by isothermally pre-saturating the sample with methane at different temperatures and checking for the subsequent release of the paraffin during a TPD ramp in inert gas. No desorption of methane or of any methane direct transformation by-product was observed at any temperature. A further TPR experiment was then carried out by feeding methane, diluted in inert gas, on the sample pre-saturated in air. The light-off temperature was ca. 350 °C (Fig. 3a), ca. 100 °C higher than that observed during the standard activity test under oxidising atmosphere. In addition, the only reaction products were CO_2 and H_2O, even under reducing reaction conditions. This confirms the high oxygen mobility within this sample and the ability of the latter to easily release oxygen to the substrate. Finally, the TPD pattern of pre-adsorbed oxygen revealed a very weak β peak around 700 °C (Fig. 3b). In our previous investigation [12] we observed that the intensity of β peak is connected with the nature of metal B, the higher its reducibility, the lower being the onset temperature of β peak. In particular, β peak appeared around 700 °C for $LaCoO_{3\pm\delta}$ and was completely absent for $LaFeO_{3\pm\delta}$ at least within the temperature limits of our experiments. By comparing those data with the present findings we can attribute the small

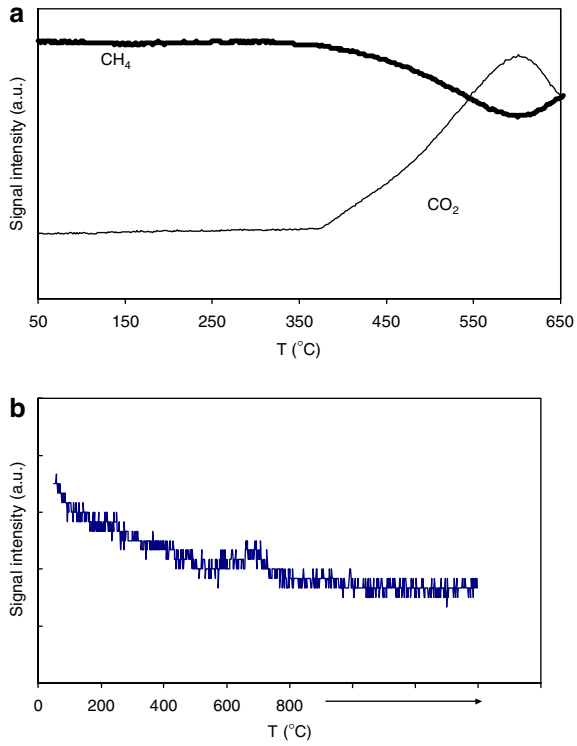

Fig. 3 (**a**) TPR analysis under reducing conditions of oxygen pre-saturated LSFC sample (Table 1); (**b**) TPD of preadsorbed oxygen. Sample LSFC (Table 1)

peak detected in our TPD experiment to oxygen released by the small fraction (20% only) of Co present in the LSFC sample. No α peak was observed for this sample (Fig. 3b).

The α peak generated at lower temperature represents the desorption of oxygen adsorbed on the catalyst surface and it is not always observable, depending on the concentration of filled anionic vacancies. In particular its onset temperature and intensity depend not only upon the nature of metal B, but also on the substitution of A with a cation of different valence [6, 8]. In particular, the unsubstituted La-ferrite did not show any α peak, while the La-cobaltite showed a weak one [12]. On the other hand, the effect of La substitution by Ce(IV) or Eu(II) on this parameter was investigated on a set of La-cobaltites [8], allowing to conclude that insertion of ions of both higher or lower valence as substitutes for La leads to the formation of the α peak, but apparently its intensity is not related to the substitution degree. Another important feature is the shift of the peak maxima, depending on the valence of the dopant, i.e. higher temperature peak maxima were observed with divalent dopants. So, in principle we would expect a more or less intense α peak for sample LSFC, in contrast with the experimental evidence.

This is only an apparent contradiction, because oxygen interaction with defective sites is more complex, involving, as already mentioned, also the nature of metal B. Indeed, EPR analysis on cobaltites clearly showed the presence of paramagnetic species, such as Co^{3+}/O_2^- pairs, and different cobalt-oxygen bond strength, depending on the nature of the dopant [8]. Moreover, spin-glass formation was reported for $La_{0.9}Sr_{0.1}CoO_{3-\delta}$, which would explain the low oxygen exchange ability of the sample and therefore its lower activity with respect to the Ce-doped catalyst, where spin-glass systems were absent [11]. Furthermore, oxygen permeation measurement on membranes of composition similar to LSFC showed that oxygen permeation increases with Co concentration, because Co(III) has a smaller ionic radius and lower metal-oxygen binding energy with respect to Fe(III). It also increases with Sr amount, since oxygen vacancies concentration increases [6]. At last, if oxygen vacancies are too concentrated, they tend to give more ordered structures, with variation of cell dimension and consequent lowering of oxygen permeability [28].

Conclusions

To conclude, many frequently counteracting phenomena accompany the substitution of both the A- and B-ion in these materials, so that it remains a very difficult task to discriminate clearly among the effect on catalytic activity of each of them. However, some general conclusions can be drawn from the present investigation:

- Ce doping at A-site of La-ferrite catalysts can totally suppress suprafacial activity and slightly enhance the intrafacial activity contribution, due to increased oxygen mobility.
- Overall catalytic activity seems however practically independent of the type of electronic conductivity (either *p*- or *n*-type).
- Mixed B-metal composition helps in modulating catalyst stability under reducing reaction conditions. High Fe content allows to optimise this parameter, but depression of oxygen mobility and hence of activity has to be prevented by a simultaneous proper doping at A-position, e.g. by Sr or Ce addition, within the solubility limits of the doping oxide.
- α Oxygen release mainly depends on La substitution, but a wide variety of parameters can influence the appearance of this peak, often leading to a-priori unpredictable behaviour.
- β Oxygen release depends strongly on B-metal reducibility.

Acknowledgements We are indebted to Pirelli Labs SpA for financial aid and for the permission to publish the present data.

References

1. Yamazoe N, Teraoka Y (1990) Catal Today 8:175
2. Peňa MA, Fierro JLG (2001) Chem Rev 101:1981
3. Fierro JLG (1993) In: Tejuca LG, Fierro JLG (eds) Properties and applications of perovskite-type oxides. M. Dekker, New York, p 195
4. Voorhoeve RJH, Remeika JP, Johnson DW (1973) Science 180:62
5. Steele BCH, Middleton PH, Rudkin RA (1990) Solid State Ionics 40/41:388
6. Teraoka Y, Zhang HM, Furukawa S, Yamazoe N (1985) Chem Lett 1743
7. Giacomuzzi RAM, Portinari M, Rossetti I, Forni L (2000) Stud Surf Sci Catal 130A:197
8. Leanza R, Rossetti I, Fabbrini L, Oliva C, Forni L (2000) Appl Catal B Environ 28:55
9. Fabbrini L, Rossetti I, Forni L (2003) Appl Catal B Environ 44:107
10. Ferri D, Forni L (1998) Appl Catal B Environ 16:119
11. Oliva C, Forni L, Vishniakov AV (2000) Spectrochim Acta Part A 56:301
12. Rossetti I, Forni L (2001) Appl Catal B Environ 33:345
13. Park S, Vohs JM, Gorte RJ (2000) Nature 404:265
14. Hibino T, Hashimoto A, Inoue T, Tokuno J, Yoshida S, Sano M (2000) Science 288:203
15. Baker RT, Metcalfe IS, Middleton PH, Steele BCH (1994) Sol St Ionics 72:328
16. Zhang HM, Yamazoe N, Teraoka Y (1998) J Mater Sci Lett 8:995
17. Beson SJ, Waller D, Kilner JA (1999) J Electrochem Soc 146:1305
18. Tsai CY, Dixon AG, Ma YH, Moser WR, Pascucci MR (1998) J Am Ceram Soc 81:1437

19. Xu Q, Huang D, Chen W, Lee J, Wang H, Yuan R (2004) Scripta Mater 50:165
20. Selected Powder X-Ray Diffraction Data, JCPDS, Swarthmore, PA, files no. 25–1060 and 37–1493
21. Forni L, Toscano M, Pollesel P (1991) J Catal 130:392
22. Campagnoli E, Tavares A, Fabbrini L, Rossetti I, Dubitsky Yu A, Zaopo A, Forni L (2005) Appl Catal B Environ 55:133
23. Szabo V, Bassir M, Van Neste A, Kaliaguine S (2003) Appl Catal B Environ 43:81
24. Szabo V, Bassir M, Van Neste A, Kaliaguine S (2002) Appl Catal B Environ 37:175
25. (a) Bard AJ, Parsons R, Jordan J (1985) Standard potentials in aqueous solutions, IUPAC, In: Dekker M (ed) New York (b) Kerr JA (2000) In: Lide DR (ed) CRC Handbook of Chemistry and Physics 1999–2000, 81st edn. CRC Press
26. Arai H, Yamada T, Eguchi K, Seiyama T (1986) Appl Catal 26:265
27. Doshi R, Alcock CB, Gunasekaran N, Carberry JJ (1993) J Catal 140:557
28. Shao Z, Dong H, Xiong G, Cong Y, Yang W (2001) J Membrane Sci 183:181